

SIMULATION AND TEST OF A NEW COAXIAL COUNTER-ROTATING AGITATOR

/ 新型同轴异转搅拌器的仿真与试验

Longlong REN^{1,2,3)}, Yuqiang LI¹⁾, Zhenxiang JING¹⁾, Yuepeng SONG^{1,2,3)}, Jing GUO^{1,2,3)}, Siwen SHEN⁴⁾¹⁾¹⁾ Shandong Agricultural University, College of Mechanical and Electrical Engineering/ China;²⁾ Shandong Provincial Key Laboratory of Horticultural Machinery and Equipment/ China;³⁾ Shandong Provincial Engineering Laboratory of Agricultural Equipment Intelligence/ China;⁴⁾ Shandong Electric Power Higher Specialised College, Department of Power Engineering/ China;

E-mail: renlonglong123@126.com

DOI: <https://doi.org/10.35633/inmateh-75-10>**Keywords:** water-fertiliser integration; coaxial counter-rotating agitator; flow field analysis; orthogonal test**ABSTRACT**

Addressing the issues of water resource wastage, low fertilizer utilization efficiency, and uneven water-fertilizer mixing in current irrigation and fertilization practices, a new type of coaxial counter-rotating agitator was designed. Based on computer numerical simulation technology, this paper simulated and analysed the agitator's modes and flow field distribution, establishing the law that governed the variation of velocity distribution within the agitator's internal flow field with changes in rotational speed. An orthogonal experimental design was employed, utilizing stirring speed, stirring duration, and submerged depth as the experimental variables, and the outcomes were subsequently analysed utilizing Design-Expert software. The findings indicated that optimal fertilizer solubility was achieved when the stirring speed was 400 r/min, the stirring time was 5 minutes, and the stirring depth was 660 mm. This study provided a theoretical basis for the design and application of the coaxial counter-rotating agitator and aided in guiding parameter selection and optimization for practical applications.

摘要

针对目前灌溉施肥中存在的水资源浪费、肥料利用率较低以及水肥混合不均匀的问题,设计了一种新型同轴异转搅拌器。本文基于计算机数值模拟仿真技术,对搅拌器的模态、流场分布进行模拟分析,确定了搅拌器内部流场的速度分布随转速变化的规律;以搅拌转速、搅拌时间和潜液深度为试验因素设计正交试验,使用 Design-Expert 软件对结果进行分析,结果表明:当搅拌速度 400 r/min、搅拌时间 5 min、搅拌深度 660 mm 时,肥料溶解度最优。本研究为新型同轴异转搅拌器的设计和运用提供了理论依据,并有助于指导实际应用中的参数选择和优化。

INTRODUCTION

Currently, agriculture accounts for more than 60% of the country's total water consumption (Dali Fang et al., 2024), and traditional irrigation techniques such as flood irrigation and manual fertilization led to inefficient water and fertilizer use, with an average fertilizer utilization rate of only 33%, which not only increased the production cost, but also exacerbated the environmental pollution problem (Yuan Hongbo et al., 2016; He Weiyuan et al., 2020). Water-fertilizer integration technology could significantly improve the simultaneous efficiency of irrigation and fertilization by delivering nutrient solution directly to plant roots through drip irrigation system (Ma Martínez Gimeno et al., 2020), and the water-fertilizer mixing efficiency was directly correlated with the utilization rate of water-soluble fertilizers (Jin Zhou et al., 2020). Inadequate dissolution of fertiliser could easily lead to clogging of irrigation pipes, and such clogging was not only difficult to remove, but also time-consuming and labour-intensive to replace the pipes, as well as significantly increasing the cost of irrigation. Therefore, it was crucial to improve the efficiency of fertiliser dissolution and to ensure that the water and fertiliser were evenly mixed.

The application of large quantities of chemical fertilizers in agricultural production raised the risk of environmental pollution, Liu Shufeng et al., (2022), investigated the effects of different solid-liquid mixing ratios, agitator forms and mixing speeds on the mixing effect, and optimized the operating parameters of the agitator and fertilizer pumps to improve the homogeneity of fertilizer mixing. Mechanical agitation was an important method to promote the homogeneity of solid-liquid mixtures. Li Tianhua et al., (2023), analysed the

¹ Longlong Ren Lecturer Ph.D. Eng.; Yuqiang Li, M.Sc. Stud. Eng.; Zhenxiang Jing, M.Sc. Stud. Eng.; Yuepeng Song, Prof. Ph.D. Eng.; Jing Guo, Prof. Ph.D. Eng.; Siwen Shen, Lecturer M.Sc. Eng.;

hydrodynamic characteristics of different fertilizer mixing modes through numerical simulation of the mixing operation of different types of fertilizers, and designed a fertilizer mixing device combining unloading reflux and mechanical agitation to realize the mixing operation of different types of fertilizers. Different forms of agitators could produce different flow fields and agitation energies, thus realizing diversified mixing effects. *Tian Yongjian, (2024)*, designed a portable air agitator, which could agitate the sediment and fix impurities at the bottom of the storage tank while blowing them to improve the homogeneity of solid-liquid mixing. *Liu Wenliang et al., (2022)*, focused on improving the uniformity of fertilizer mixing, optimized and improved the fertilizer mixing components, and made use of the mixer's own structure to make the water and fertilizer fully mixed. *Zhang Shuai et al., (2018)*, designed a high-efficiency fertilizer mixer to analyse the flow field distribution diagram of different mixing speeds, and the fertilizer mixer produced more disturbed and turbulent flow inside the fertilizer mixer when the mixing speed was greater than the critical mixing speed, which could effectively improve the effect of fertilizer mixing. *Li Lei., (2024)*, designed an energy-saving axial flow mixer by setting the paddles in a circular arc shape and the arc side set diagonally downward, which enhanced the degree of turbulence in the axial and radial directions, so as to make the mixing effect better. When designing a mixing and blending device for fertilizers, it was crucial to ensure dissolution efficiency and mixing homogeneity of the fertilizers, and rational design of the mixing device was the key to achieving this goal (*Dang Lingui et al., 2013*).

This paper evaluated a newly designed mixer with a novel shape, explored the velocity distribution of the flow field inside the agitator with the change of rotational speed through computer simulation, compared with the coaxial co-rotating agitator, verified the superiority of the design of the fertilizer mixer, and obtained the optimal operating parameters of the agitator through design experiments and parameter optimization.

MATERIALS AND METHODS

Structural design of the fertilizer mixing unit

Selection of fertilizer mixing drum with an inner diameter of 600 mm and a height of 1,000 mm. According to the relevant literature and the requirements of the mechanical design of mixing equipment, combined with the relevant design specifications and empirical formulas, through the calculation of the overall size of the agitator, the relevant values were obtained:

$$d = (0.2 \sim 0.5)D \quad (1)$$

$$h = 0.02 d \quad (2)$$

$$S = 0.66 D \quad (3)$$

where: D - inner diameter of fertilizer mixing drum, mm; d - diameter of mixing paddle, mm; h - thickness of mixing paddle, mm; S - agitator submergence depth; mm;

By calculating the dimensional parameters of the agitator through the above formula, the diameter of the stirring paddle was set to 200 mm, the thickness of the stirring paddle was 4 mm, and the submerged depth of the agitator was 660 mm. Common agitators on the market are single-steering single-paddle axial-flow agitators, which have mediocre mixing effect and cannot form a turbulent field to dissolve fertilizers very well. Therefore, based on the shortcomings of the existing agitator, a new type of coaxial counter-rotating agitator was designed by making the stirring direction bidirectional and incorporating double paddles. A three-bladed propeller agitator paddle was used, providing improved mixing efficiency and enhanced hydrodynamic characteristics. The three-blade paddle could produce uniform radial and axial flow, improved mixing efficiency and reduced dead zone, while balancing the mechanical vibration in the mixing process and enhancing the stability of the system. The inclination angle of the agitator designed for 30° could be adapted to most of the equipment structure requirements of the water and fertilizer integration machine, under the condition of the same power consumption, small diameter, high speed agitator, the power was mainly consumed in the turbulent pulsation, which was conducive to the microscopic mixing.

The upper mixing paddle of the coaxial counter-rotating agitator was connected to the outer sleeve, and the lower mixing paddle was connected to the centre shaft, which was designed to be easy to install and prevent relative sliding in the working process. The upper and lower mixing paddles were connected by C-type coupling. When the mixer was working, the upper bevel gear and the lower bevel gear were synchronized to rotate in the reverse direction, which made the upper and lower mixing paddles rotate in the reverse direction coaxially. Realizing the effect of a composite cyclonic flow field in a single device could create a larger turbulence distribution during mixing and improve the homogeneity of mixing and blending (*Hua Jian et al., 2023*), the final design is shown in Fig. 1. Fig. 2 shows the overall structural diagram of the fertilizer mixer, and Fig. 3 shows the structure of the mixing paddle.



Fig. 1 - Coaxial counter-rotating agitator

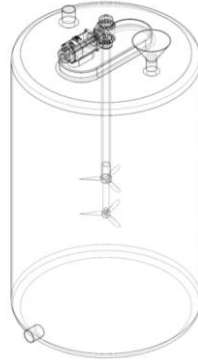


Fig. 2 - Overall structure of the fertilizer mixer

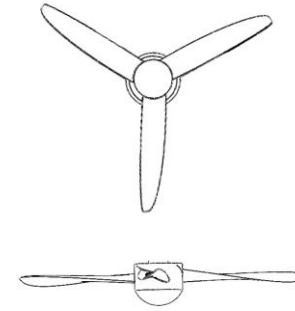


Fig. 3 - Mixing paddle

Calculation of critical stirring speed of the agitator

Agitation had a limited effect on the mass transfer coefficient, mainly by promoting the suspension of solid particles to increase the solid-liquid interface, and thus improved the mass transfer efficiency. When the complete suspension of particles was achieved, it was no longer obvious to increase the stirring intensity to improve the mass transfer efficiency. For the process of dissolving solids, the bottom of the particles can be suspended, without the need to achieve a complete uniform distribution of the liquid phase. In view of this, it was crucial to determine the critical stirring speed of the mixing equipment, which depended on the density difference between the solid and liquid phases, the liquid density, the solids concentration, the liquid viscosity, the physical properties such as particle size, and the geometrical relationship between the mixing vessel and the agitation device. Based on the formula for calculating the critical stirring speed published by Zwietering, it was possible to determine the appropriate stirring speed, avoiding unnecessary energy consumption:

$$N_c = Kd^{-0.85} \nu^{0.1} d_p^{0.2} \left| g \frac{\rho_p - \rho}{\rho} \right|^{0.45} \left| 100 \times \frac{\rho_p \phi_v}{\rho(1 - \phi_v)} \right|^{0.13} \quad (4)$$

where: N_c - critical RPM; K - equation constant, the propeller impeller is approximately $2.57 \sim 3.19(D/d)0.80 \sim 0.86$; D - inner diameter of fertilizer mixing drum, m; d_p - solid particle diameter, m; ϕ_v - solid volume fraction; ρ - density of liquids, kg/m^3 ; ρ_p - density of solid particles, kg/m^3 ; ν - kinematic viscosity of liquids, m^2/s ; d - diameter of mixing paddle, m; g - gravitational acceleration, m/s^2 ;

The majority of the parameters in the above equation were determined by the calculation of the specific dimensions of the mixer in the paper, and according to the study of *Yang Xiaozhen et al., (2014)*, it was known that the density of the water-fertiliser mixing liquid was 1150 kg/m^3 and its kinematic viscosity was $0.0016 \text{ m}^2/\text{s}$. The data provided by *Guo Shanming et al., (2017)*, pointed out that the particle diameter of the general-purpose water-soluble fertilisers was 2 mm , and its density was 1335 kg/m^3 . Based on these parameters, the critical stirring speed (N_c) was calculated to be approximately 398.28 r/min . The critical stirring speed (N_c) of the fertiliser mixer was calculated to be approximately 398.28 r/min , and this result was informative for subsequent comparative class studies.

Simulation modelling and meshing of agitator

In computer simulation analysis, meshing was crucial because proper meshing could improve simulation accuracy and reduce the time required for computation (*Zhang Yubin et al., 2018*).

Through COMSOL Multiphysics software, the simulation model used a tetrahedral mesh and the rotating part of the agitator was refined to ensure higher simulation accuracy (*An Bo et al., 2023*). The histogram of the mesh quality showed a normal distribution, ensuring uniformity and proper size distribution of the mesh. Figure 4 shows the grid details of the flow field analysis of the agitator and fertilizer mixing tank.

After the meshing was completed, the quality of the grid was viewed through the statistical information under the grid (mesh) component, where the agitator grid diagram in Figure 3 had a cell count of $187,122$, and the fertilizer mixing tank grid diagram had a cell count of $850,624$ for the statistical information of the domain cells.



Fig. 4 -Agitator grid figure; flow field analysis grid diagram of fertilizer mixing tank

Modal analysis of coaxial counter-rotating agitator

The high speed of rotation during agitator operation led to vibration. To ensure the stability of the equipment, modal analysis was essential to reveal the vibration characteristics. Modal analysis was designed to identify the inherent vibration modes of an object based on a fixed structural shape and constraints. Based on the established model and constraints imposed (Liu Shuangxi et al., 2020), modal analysis could be performed to obtain the first six modal frequencies of the agitator, the first six orders of modal diagrams were shown in Fig. 5.

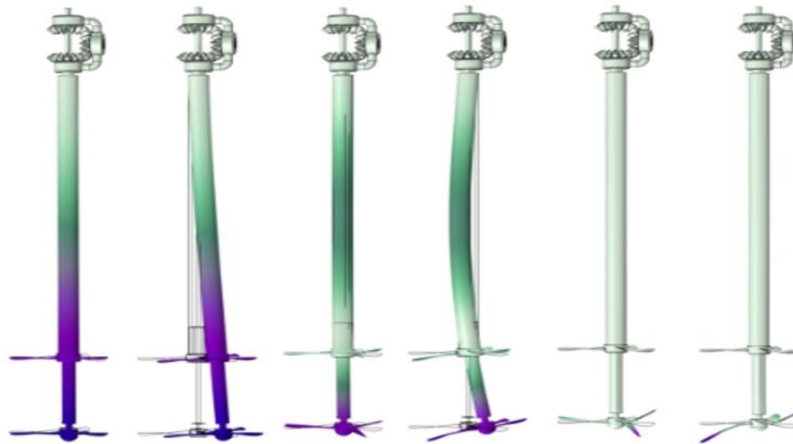


Fig. 5 - First six modes

Simulation analysis of the flow field of a coaxial counter-rotating agitator

In the study of fluid dynamics, velocity vector diagram was an important tool to reveal the dynamic trend, state and change of flow direction of the fluid in the flow field (Jin Yu et al., 2023). In this study, numerical simulation was used to simulate the flow at different rotational speeds, specifically analysing the velocity field distribution in the central profile of the fertilizer mixer at rotational speeds of 200, 300, 400 and 500 r/min, respectively.

The spatial distribution characteristics of the flow velocity could be observed visually through the generated velocity clouds. Comprehensive comparison of these velocity cloud maps enabled this study to explore in depth the law of the velocity distribution of the flow field inside the agitator as a function of the rotational speed, and to determine the optimal operating rotational speed accordingly.

Prototyping and design of experiments

In this paper, through mechanical design as well as simulation analysis, the coaxial counter-rotating agitator was designed and the prototype object was machined, as shown in Fig. 6. The main components of the agitator, such as the active teeth, motor, coupler, outer sleeve, lower stirring paddle, upper stirring paddle, lower follower teeth, centre shaft, upper follower teeth, etc., are indicated in the figure. The overall size and length of the agitator was consistent with the previous design model, while the structure was compact and the components had good working stability. In the actual production process, in order to save production costs, a fixed-speed motor with defined parameters could be chosen, which could effectively meet the production requirements and would not require frequent adjustment of the agitator's stirring speed.

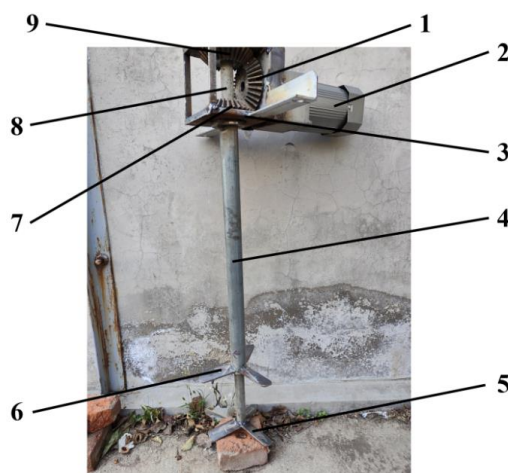


Fig. 6 -New coaxial counter-rotating agitator

1. Driving teeth, 2. Motor, 3. Coupler, 4. Outer sleeve, 5 down stirring paddle, 6. Upper stirring paddle, 7. Lower driven teeth, 8. Centre shaft, 9. Upper driven teeth

In this study, in order to determine the optimal agitation conditions, the Box-Behnken design method was used with stirring speed, stirring time and submergence depth as independent variables and electrical conductivity (EC) as the response variable. By implementing a three-factor, three-level orthogonal experimental design, it was aimed to find the optimal combination of stirring speed (A, a), stirring time (B, b) and agitator submergence depth (C, c). The experimental conditions were designed as follows: the N, P, and K ratio of the mixed fertilizer was 20% ~ 20% ~ 20%. For the test, 1000 g of fertilizer was selected and mixed with 100 L of aqueous solution under different test conditions. After the mixing was completed, 200 ml of the fertilizer aqueous solution was taken out and its concentration was determined using a portable PH/EC tester. In this case, electrical conductivity (EC value) was used as a measure of the solubility of the fertilizer. Fig.7 shows the physical picture of the composite fertilizer and Fig. 8 shows the test site.



Fig. 7 - Physical Map of Fertilizer



Fig. 8- Pilot test site

The experimental range of stirring speed was set at 300 to 500 r/min, based on the results of previous hydrodynamic simulations. The stirring time was selected from 3 to 7 minutes to ensure adequate dissolution of the fertilizer and reasonable energy consumption. The submerged depth of the agitator was set between 610 and 690 mm based on previous calculations. Table 1 demonstrated the experimental factors with their corresponding coded values. This experimental design and parameter selection was devoted to evaluate the effectiveness of the new coaxial counter-rotating agitator in the fertilizer mixing process, so as to provide theoretical and experimental support for the optimization of the fertilizer mixing process.

Table 1

Correspondence between Test Factor Level and Coded Value in Stirring Process

Coded value	Stirring speed A / (r/min)	Stirring time B / min	Agitator submergence depth C / mm
-1	300	3	610
0	400	5	650
1	500	7	690

RESULTS

Analysis of agitator simulation results

According to the results of the modal analysis in Table 2, the fundamental frequency of the agitator was 38.57 Hz, which was the lowest among all modes. Considering that the operating frequency interval of the speed-regulated motor was 0-500 r/min, this corresponded to a vibration frequency of 0-8.34 Hz. Since this frequency was much lower than the first order modal frequency of the agitator, the effect of other external excitation frequencies on the fertilizer mixing tank could be neglected. Literature indicates that the lower order modes had a more significant effect on the vibration of the equipment, while the effect of the higher order modes gradually decreases (Liu Shuangxi et al., 2020). In summary, the highest frequency of external excitation was significantly lower than the lowest mode of the mixer, which means that the agitator had good anti-vibration performance and would not enter into resonance due to external excitation, meeting the design specification requirements.

Table 2

Sixth-order mode of blender						
ORDER	1	2	3	4	5	6
FREQUENCY / Hz	38.57	41.11	250.42	256.28	449.16	449.41

Fig. 5 showed that the vibration pattern of the agitator was mainly divided into the vibration of the stirring rod and the vibration of the stirring paddle, in which the vibration pattern corresponding to the first, second, third and fourth order modes was mainly the left and right oscillation of the stirring rod. The vibration mode corresponding to the fifth and sixth order modes was mainly the up and down swinging of the agitator paddle, while the agitator was mainly operated by the central shaft and outer sleeve rotating around the centre with the same direction and speed. The vibration characteristics of the agitator were mainly expressed as torsional vibration in the direction of the central axis, which was different from the transverse and vertical vibration modes.

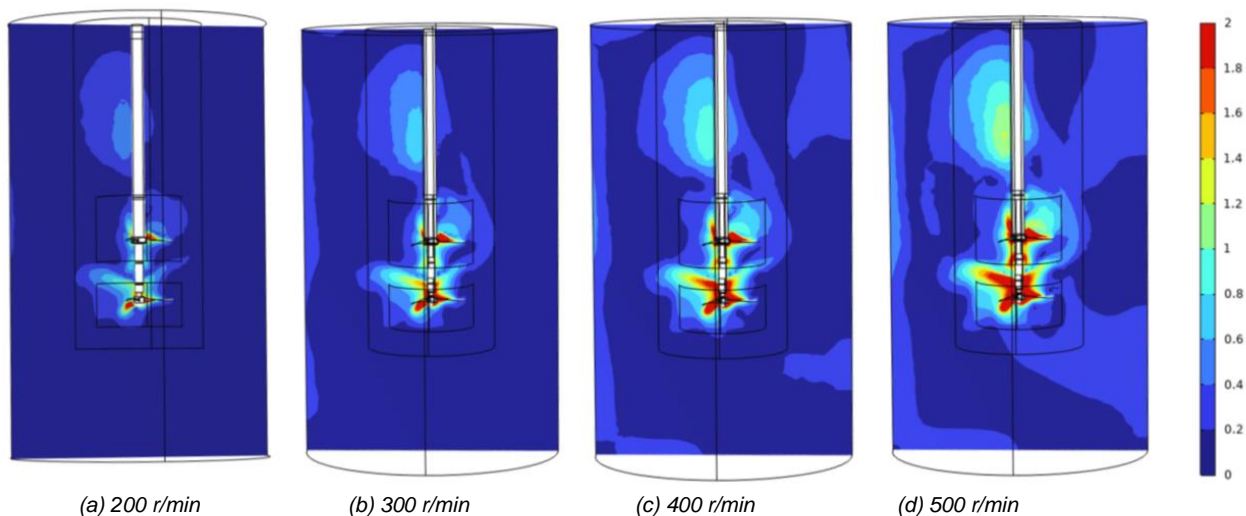


Fig. 9 - Speed cloud picture of agitator at different speeds

From Fig. 9, it could be observed that at critical speeds lower than 400 r/min, the velocity was higher near the rotating paddle and lower at the periphery away from the rotor. The velocity distribution in this region was more uniform and lacked a significant velocity gradient, resulting in a weakening of the interlayer flow, which was not conducive to the development of turbulence, thus affecting the dissolution and mixing efficiency of the fertilizer.

When the rotational speed was higher than the critical rotational speed of 400 r/min, it was observed that the overall velocity cloud map showed a similar pattern, with a larger value of velocity in the rotating region of the agitator's stirring paddles, and the overall velocity in the fertilizer mixing drum showed the distribution characteristics of the middle being the highest, the edge the second highest, and the mezzanine being the lowest, which formed an obvious middle-low-high velocity distribution. This velocity distribution effectively enhanced the relative motion between the liquid layers, and this frequently changing medium-low-high velocity distribution formed a complex flow field distribution, which promoted turbulence and was conducive to the dissolution of the fertilizer.

Analysing the velocity clouds under different speed conditions, it could be seen that: under the condition of lower than critical agitation speed, the flow field of the agitator showed a single flow pattern, and the turbulence distribution was restricted, which limited the dissolution efficiency of the fertilizer.

In contrast, when the speed was higher than the critical agitation speed, the distribution of the flow field became more complex, the value of the velocity in the rotating area of the agitator's mixing paddles was larger, and the overall velocity in the fertiliser mixing drum showed the distribution characteristics of the highest in the middle, the second on the edge, and the lowest in the mezzanine layer, which phenomenon improved the shear action and circulation characteristics inside the fluid and thus accelerated the dissolution mechanism of the fertilisers. With the increase of velocity, the velocity vector field and velocity isosurface map mainly reflect the growth of velocity amplitude, while the overall distribution pattern of velocity was kept relatively consistent with the trend of vector change.

Therefore, after the speed exceeded the critical stirring speed, increasing the rotational speed had less effect on the distribution of the flow field, but the velocity value would increase. After comparison and analysis, both 400 r/min and 500 r/min speed could meet the requirements. Considering the overall power consumption, the rotational speed should be reduced as much as possible to improve the energy efficiency while generating a good flow field distribution. Therefore, 400 r/min is finally selected as the optimum speed for the new coaxial counter-rotating agitator.

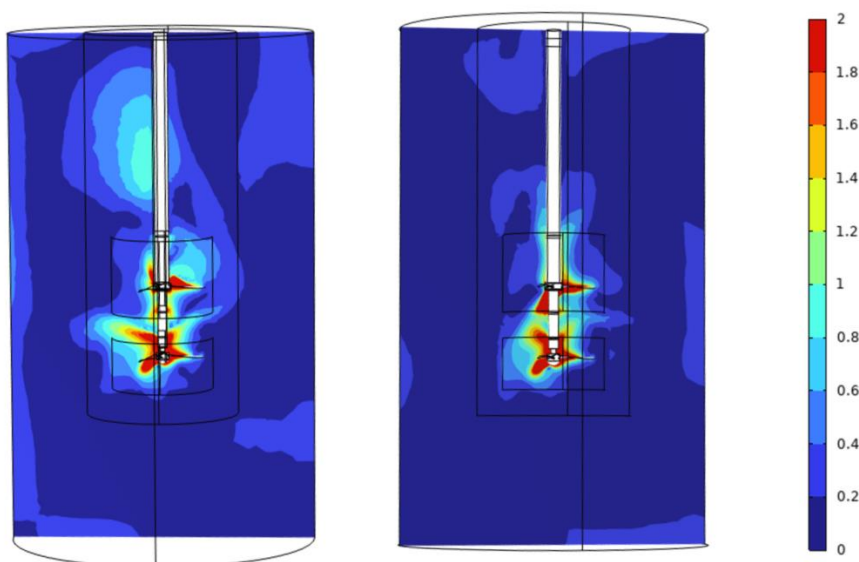


Fig. 10 - Velocity distribution at 400 r/min under coaxial differential rotation and coaxial simultaneous rotation

The simulation results in Fig. 10 showed that the overall flow velocity distribution of the coaxial counter-rotating agitator was significantly better than that of the coaxial co-rotating agitator when the rotational speed was 400 r/min. Due to the fact that the stirring blades of the coaxial co-rotating stirrer rotated in the same direction, it resulted that the flow velocity in the flow field was concentrated in the rotating region of the stirring blade, and the mobility was insufficient. Therefore, this situation was not conducive to the dissolution of fertiliser and other processes. The coaxial counter-rotating agitator produced stronger vortex and turbulence effects due to the opposite direction of rotation of the agitator paddles. Such flow characteristics were conducive to diffusion and mixing, making the process of dissolving fertiliser more complete and rapid.

Through numerical simulation analysis, the multi-dimensional flow field structure produced by the coaxial counter-rotating agitator could promote the effective contact between the fertiliser particles and the solvent, which increased the surface area of dissolution, and was conducive to improving the dissolution rate and efficiency

Regression modelling and analysis of variance

An important indicator for assessing the results of the working parameters was the electrical conductivity (EC value) of the fertilizer solution, which was obtained by removing 200 ml of aqueous fertilizer solution from the fertilizer mixing drum after mixing and measuring its concentration using a portable PH/EC tester. In accordance with the principles of Box-Behnken experimental design, 17 sets of experiments on fertilizers were executed in this study and the corresponding data were collected. The experimental program and its results were summarized in Table 3.

Table 3

Fertilizer Mixing Test Scheme and Result

No	Stirring speed A/(r/min)	Stirring time B/min	Agitator submergence depth C/mm	Fertiliser EC M/(us/cm)
1	0	1	1	10840
2	0	0	0	11430
3	0	-1	-1	10380
4	0	0	0	11480
5	0	-1	1	10240
6	1	-1	0	10620
7	-1	0	1	10110
8	0	0	0	11450
9	-1	-1	0	9780
10	1	0	-1	10940
11	0	0	0	11460
12	0	0	0	11430
13	-1	1	0	10480
14	1	1	0	11090
15	0	1	-1	10920
16	1	0	1	10710
17	-1	0	-1	10060

Note: m1, m2 and m3 are the corresponding coded values of M1, M2 and M3, the same as below.

A quadratic regression model was obtained as a result of analysing and processing the experimental data shown in Table 3 by entering them into the Design Expert software. The model describes the relationship between the electrical conductivity (EC value) of the water-soluble fertilizer obtained after dissolving the fertilizer and the coded values of the three variables: agitation speed, agitation time, and agitator submergence depth. The quadratic regression equations obtained from the EC value of the water fertilizer solution and the coded values of the three influencing factors, stirring speed, stirring time and agitator submergence depth, respectively, were:

$$M = 11450 + 366.25a + 288.875b - 49.875c - 57.5ab - 70ac + 15.25bc - 548.875a^2 - 408.625b^2 - 446.125c^2 \tag{5}$$

The results obtained from the analysis of variance (ANOVA) of the regression equation for fertilizer solubility using Design Expert software showed that the P-values of all the factors in the model were significantly below the 0.05 threshold. And the P-values of three variables, namely, agitation speed, agitation time and submerged depth of agitator were well below 0.01, which characterizes the regression model as being extremely statistically significant. The magnitude of the F-statistic further indicated the importance of these variables in the model, manifesting their impact on the amount of fertilizer dissolved. A larger F value implies a stronger influence. Accordingly, among the factors examined, agitation speed had the most significant effect on fertilizer solubility, followed by agitation time, and then submerged depth of the agitator.

Table 4

Analysis of variance

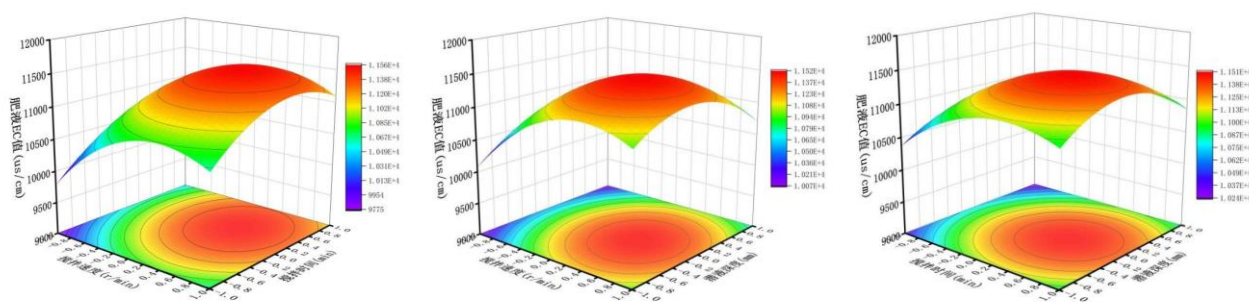
Source of variance	Square sum	Degrees of freedom	Mean square	F-value	P-value	Significance
Model	4.927e6	9	5.474e5	1735.75	< 0.0001	**
a	1.073e6	1	1.073e6	3402.46	< 0.0001	**
b	6.676e5	1	6.676e5	2116.69	< 0.0001	**
c	19900.13	1	19900.13	63.10	< 0.0001	**

Source of variance	Square sum	Degrees of freedom	Mean square	F-value	P-value	Significance
ab	13225.00	1	0.023	41.93	0.0003	**
ac	19600.00	1	0.01	62.14	0.0001	**
bc	930.25	1	0.016	2.95	0.1296	
a2	1.268e6	1	1.268e6	4021.90	< 0.0001	**
b2	7.031e5	1	7.031e5	2229.12	< 0.0001	**
c2	8.38e5	1	8.380e5	2657.04	< 0.0001	**
residual	2207.75	7	315.39			
lost proposal	407.75	3	135.92	0.3020	0.8236	
errors	1800.00	4	450.00			
sum	4.929e6	16				

Note: *means significant, $p < 0.05$; **means significant, $p < 0.01$

Two-factor interaction effect analysis and parameter optimization

Based on the results obtained from the analysis of the above regression equation, the effect of the remaining factors on the solubility of the fertilizer will be further investigated by arbitrarily selecting the level of one of the factors to be zero. By applying Design Expert software, the response surface for the interaction effects was derived as shown in Fig. 11.



(a) stirring speed versus stirring time response surface (b) stirring speed versus submerged liquid depth response surface (c) stirring time versus submerged liquid depth response surface

Fig. 11- Corresponding surfaces for the effect of interacting factors on test metrics

When observing the images, it was found that the two-factor response surface morphology of different fertilizers showed remarkable consistency, and there was also an essential similarity in the influence pattern of each factor. First of all, through Figure 11a it was noticed that the solubility of fertilizers tended to increase with the increase of time under the condition that the stirring speed was kept constant. However, the effect on the solubility gradually decreased with the continuous increase of time. In the case where the stirring time was kept constant, the solubility of the fertilizer tended to increase as the stirring speed increased. The effect on solubility gradually decreased as the speed was increased to a certain level. Observation of Fig. 11c reveals a similar pattern, which also showed a tendency of decreasing and then increasing as the depth of the submerged liquid increased.

Finally, observation of Figure 11b reveals that the solubility of the fertilizer tended to increase as the stirring speed increased while the depth of the submerged liquid was kept constant, but once the speed was increased to a certain level, its effect on the solubility gradually diminished. The effect of stirring time also showed a similar pattern. Therefore, the above analysis showed that the effects of stirring time, stirring speed and submerged liquid depth on the solubility of fertilizers had similar regular trends. Under well-mixed conditions, continuing to increase the stirring speed made a decreasing contribution to the dissolution of the fertilizer, consistent with the simulation data. Therefore, optimizing the stirring speed can reduce energy consumption while ensuring mixing efficiency. Similarly, the increase in dissolution rate by extending the agitation time had a marginal effect and was limited by the inherent solubility of the fertilizer.

Selecting the appropriate stirring time was a key factor in reducing energy consumption and improving operational efficiency.

The depth of submerged liquid had a significant effect on the solubility of fertilizer, showing a non-linear relationship. The undissolved amount of fertilizer decreased and then increased as the submerged depth increased. This phenomenon would be due to the fact that too deep a submerged depth would result in the flow field generated by agitation at the bottom of the container, although it was ideal, but its effect could not be effectively extended to the upper layer of the liquid; and when the submerged depth was insufficient, the flow field could not reach the bottom of the container adequately.

Therefore, optimizing the submerged liquid depth was a key factor to improve the efficiency of fertilizer dissolution.

Combining the above factors, global multi-objective optimization was carried out, and the fertilizer solubility was taken as the objective function, and the stirring speed, stirring time and submerged liquid depth were optimally designed. The best combination of each parameter was available through the optimization mathematical model equation, according to the optimization mathematical equation :

$$\begin{cases} \max M = f_1 & A, B, C \\ s.t. \begin{cases} A \in 300, 500 \\ B \in 3, 7 \\ C \in 610, 690 \end{cases} \end{cases} \quad (6)$$

where: A, B, and C were the actual values corresponding to stirring speed, stirring time, and agitator submergence depth, respectively.

In order to obtain the optimal parameter combinations, Design expert software would be applied to solve the optimization. Finally, Table 5 would present the optimal operating parameter combinations of the agitator.

Table 5

Table 4 Optimal combination of operating parameters			
Type	Optimum stirring speed / (r/min)	Optimum stirring time /min	Optimum Submersible Depth /mm
Theoretical	394.3	5.31	651.64
Actual value	400	5	660

To ensure the feasibility of the theoretically optimized values in practical applications, rounding was performed and experimentally verified. The results showed that the optimal agitation parameters were 400 r/min, 5 min stirring time, and 660 mm agitator submerged liquid depth.

CONCLUSIONS

(1) A new type of coaxial counter-rotating agitator was designed and the results of modal analysis showed that the agitator had good vibration performance and did not cause equipment resonance, which was in line with the design expectations.

(2) The field simulation analysis showed that when the stirring speed exceeded the critical agitation speed threshold, the fluid flow was complicated, the speed in the agitation zone was higher, and the velocity distribution in the fertilizer mixing drum was characterized as the highest in the middle, the second highest at the edge, and the lowest in the mezzanine. In order to improve energy efficiency, 400 r/min was finally determined as the optimal speed.

(3) The Box-Behnken design method was used to optimize the working parameters, and quadratic regression analysis was used to investigate the effects of stirring speed, time and agitator submerged depth on the solubility of fertilizers, and it was found that the solubility of fertilizers increased with the increase of stirring speed and time, but the positive effect was weakened beyond the specific threshold, and the relationship between the submerged depth of the agitator and the solubility showed a nonlinear correlation. The optimal working parameters were stirring speed of 400 r/min, stirring time of 5 min, and submerged depth of 660 mm.

ACKNOWLEDGEMENT

We are very grateful to all the authors for their support and contribution with the manuscript. This work is partly supported by: Key R&D Program of Shandong Province, China" (2024TZXD045, 2024TZXD038);

Innovation Team Fund for the Fruit Industry of Shandong's Modern Agricultural Technology System (SDAIT-06-12); The State Key Laboratory of Mechanical System and Vibration (Grant No. MSV202002), and the Modern Agriculture Coarse Grain Industry Technology System Project of Shandong Province (SDAIT-15-05).

REFERENCES

- [1] An, B., Meng, X. Y., Yang, S. J., Sang, W. M., (2023). Study of local mesh refinement LBM algorithm for non-uniform rectangular grids. *Journal of Mechanics*, vol.55(10), pp. 2288-2296.
- [2] Dang, L G., Guo, S X., Wang, D. B., Zhang, S. G., Cao, H. L., (2013). Numerical study of agitation characteristics of different combined paddle agitators, *Journal of Zhengzhou University: Engineering Edition*, vol.34 (03), pp. 59-62.
- [3] Fang, D. I., Wang, J., Liu, J. J., Lou, Y. Z., (2024). Spatial and Temporal Differentiation of Agricultural Water Use Efficiency and Its Influencing Factors Under the Combination of Multiple Models. *Water Saving Irrigation*, pp. 105-113.
- [4] Guo, S. M., Liu, J. P., (2017). Commonly used fertilisers and scientific fertilization technology for greenhouse vegetables, *Agriculture and Technology*, vol.37 (24), pp. 32-32.
- [5] Hua, J., Li, W., Lu, Z. P., Zhan, L. B., Huang, T. C., (2023). Study on solid-liquid mixing uniformity in double-layer paddle mixing tank [J]. *Science, Technology and Engineering*, vol.23 (28), PP. 80-90.
- [6] Jin, Z., Zhang, J., Guo H. Y., Hu, Y. M., Chen, X. Y., Huang, H., Wang, H. Y., (2020). Development and testing of intelligent sensing and precision proportioning system of water and fertilizer concentration. *Smart Agriculture*, vol.2 (2), pp. 82-93.
- [7] Jin, Y., Zhao, L. X., Xu, B. R., Zhang, X. G., et al., (2023). Flow field characteristics of a cyclone separation column under vibration conditions. *Chemical Engineering*, vol.51(11);
- [8] Li, L., (2024). Energy-saving axial flow mixer. Patent. CN202410985251.3 CHINA Li, T. H., Zhang, S. Q., Zhang, C. F., et al., (2023). Research and experiment on efficient mixing modes of different forms of water and fertilizer. *INMATEH Agricultural Engineering*, vol.70 (2), pp. 278-298.
- [9] Liu, S. F., Lu, Z. Q., Shi, X. P., et al., (2022). Analysis and design of solid-liquid mixed fertilizer device for organic fertilizer on solid-liquid two-phase flow. *INMATEH Agricultural Engineering*, vol.66 (1), pp. 167-181.
- [10] Liu, S. X., Xu, C. B., Zhang H. J., Zhang, C. F., Liu, X. M., (2020), Optimised design and test of orchard open furrow fertiliser machine frame. *Journal of Agricultural Machinery*, vol.51 (S1), pp. 113-122.
- [11] Liu, W. L., Yang, R. B., Pan, Z. G., et al., (2025). Design and experimental study of water-fertilizer integrated fertilizer mixer in large fields. *Journal of Agricultural Mechanization Research*, vol.47 (2), pp. 139-145.
- [12] Martínez-Gimeno M A., Jiménez-Bello M A., Lidón A, Manzano J., Badal E., Pérez-Pérez J G., Bonet L., Intrigliolo D S and Esteban A., (2020). Mandarin irrigation scheduling by means of frequency domain reflectometry soil moisture monitoring. *Agricultural Water Management*, vol.235, issue.5, pp. 234-241.
- [13] Song, Y. P., Zhang, S., Li, T. H., Gao, D. S., Fan, G. J., (2018). Design and numerical simulation analysis of orchard fertilizer mixer. *Transactions of the Chinese society for Agricultural Machinery*, vol.49 (S1), pp. 181-188.
- [14] Tian, Y. J., Hui, T., Li, X. J., Zhang, A., Bai, Y. J., (2024). *A portable air agitator*. Patent. CN202323497341.8. China
- [15] Wang, F. H., Zhang, C. H., Wang, G. Q., Jiang, L. Y., Liu, H., (2024). Numerical simulation and performance analysis of granular fertilizer agitator in greenhouse. *Journal of Agricultural Mechanization Research*, vol.45 (10), pp. 60-68.
- [16] Wu, X. B., Gong, F., Ye, Y., (2023). Regional differences and convergence of green efficiency of agricultural water use in China. *China Rural Water Conservancy and Hydropower*, vol.6, pp.196-201.
- [17] Yuan, H.B., Li, L., Wang, J.H., Wang, H. H., N. A. Sigrimis., (2016). Design and testing of greenhouse water-fertiliser-integrated nutrient solution control equipment. *Journal of Agricultural Engineering*, vol.32, issue 8, pp.27-32.
- [18] Zhang, Y., Zhang, N., Wang, Y. Q., Liu, X. H., (2014). Effects of drip irrigation on the growth, yield and quality of watermelon in greenhouse, *Journal of Agricultural Engineering*, vol.30 (7), pp. 109-118.
- [19] Zhang, Y. B., Wei, Z. Y., Hu, Y., (2018), Design and numerical simulation of water-fertiliser mixer, *Agricultural Mechanisation Research*, vol. 40 (3), pp. 33-36.